Circulating mitochondrial *N*-formyl peptides contribute to secondary nosocomial infection in patients with septic shock

Woon Yong Kwon[a,b,1], Gil Joon Suh[a,b], Yoon Sun Jung[b], Seung Min Park[c], Subi Oh[c], Sung Hee Kim[b], A. Rum Lee[b], Jeong Yeon Kim[b], Hayoung Kim[b], Kyung Ah Kim[d], Young Kim[d], Byoung Choul Kim[d,e], Taegyun Kim[b], Kyung Su Kim[b], Kiyoshi Itagaki[f], and Carl J. Hauser[f]

[a]Department of Emergency Medicine, Seoul National University College of Medicine, Seoul 03080, Republic of Korea; [b]Department of Emergency Medicine, Seoul National University Hospital, Seoul 03080, Republic of Korea; [c]Department of Medicine, Seoul National University College of Medicine, Seoul 03080, Republic of Korea; [d]Department of Bioengineering and Nano-Bioengineering, Incheon National University, Incheon 22012, Republic of Korea; [e]Division of Nano-Bioengineering, Incheon National University, Incheon 22012, Republic of Korea; and [f]Department of Surgery, Beth Israel Deaconess Medical Center/Harvard Medical School, Boston, MA 02215

Edited by Paul Kubes, University of Calgary, Calgary, AB, Canada, and accepted by Editorial Board Member Carl F. Nathan March 3, 2021 (received for review September 5, 2020)

Secondary infections typically worsen outcomes of patients recovering from septic shock. Neutrophil [polymorphonuclear leukocytes (PMNs)] migration to secondarily inoculated sites may play a key role in inhibiting progression from local bacterial inoculation to secondary infection. Mitochondrial *N*-formyl peptide (mtFP) occupancy of formyl peptide receptor-1 (FPR1) has been shown to suppress PMN chemotaxis. Therefore, we studied the association between circulating mtFPs and the development of secondary infection in patients with septic shock. We collected clinical data and plasma samples from patients with septic shock admitted to the intensive care unit for longer than 72 h. Impacts of circulating nicotinamide adenine dinucleotide dehydrogenase subunit-6 (ND6) upon clinical outcomes were analyzed. Next, the role of ND6 in PMN chemotaxis was investigated using isolated human PMNs. Studying plasma samples from 97 patients with septic shock, we found that circulating ND6 levels at admission were independently and highly associated with the development of secondary infection (odds ratio = 30.317, 95% CI: 2.904 to 316.407, $P = 0.004$) and increased 90-d mortality (odds ratio = 1.572, 95% CI: 1.002 to 2.465, $P = 0.049$). In ex vivo experiments, ND6 pretreatment suppressed FPR1-mediated PMN chemotactic responses to bacterial peptides in the presence of multiple cytokines and chemokines, despite increased nondirectional PMN movements. Circulating mtFPs appear to contribute to the development of secondary infection and increased mortality in patients with septic shock who survive their early hyperinflammatory phase. The increased susceptibility to secondary infection is probably partly mediated by the suppression of FPR1-mediated PMN chemotaxis to secondary infected sites.

sepsis | neutrophils | infections | nosocomial | formyl peptide

Secondary nosocomial infections are thought to reflect sepsis-induced immune paralysis, and they clearly worsen clinical outcomes in patients recovering from septic shock. Current concepts of sepsis management therefore emphasize the prevention of secondary immune paralysis (1–3). Neutrophil (polymorphonuclear leukocyte, PMN) migration to secondarily inoculated sites in response to chemoattractants is a critical aspect of innate immune responses to secondary infection (4, 5). The binding of chemoattractants to surface G protein–coupled receptors (GPCRs) induces the depletion of endoplasmic reticulum calcium stores (ER calcium depletion) and subsequent cytosolic calcium influx, which generates PMN polarity and chemotaxis in response to GPCR agonists (6–10).

Mitochondrial damage–associated molecular patterns (mtDAMPs) are released from injured tissues (11–14). MtDAMPs express at least two critical inflammatory molecular signatures: mitochondrial *N*-formyl peptides (mtFPs) and mitochondrial DNA (mtDNA) (15, 16). MtFPs bind to formyl peptide receptor-1 (FPR1) on the PMN membrane, desensitizing FPR1 and other GPCRs via internalization of the receptors (11, 17–20). This step blocks the binding of chemoattractants to a broad range of GPCRs potentially suppressing PMN migration toward bacterial inoculation sites (11, 17–20). Our previous studies have shown that mtDAMPs released by extrapulmonary injuries can reduce bacterial clearance and so increase secondary pneumonia by suppressing PMN chemotaxis toward secondary stimuli and that FPR1 blockade prevented down-regulation of PMN chemotaxis by preserving non-FPR1 GPCRs after injury (11, 21, 22).

Septic shock commonly induces multiorgan injury both directly via tissue inflammation and secondarily via hypoperfusion (23–25). Both of these events can result in mtDAMP release into the circulation. Unlike the situation early after injury though, in septic shock, it's well-known that ongoing systemic inflammation

Significance

Septic shock commonly leads to multiorgan injury both directly via tissue inflammation and secondarily via hypoperfusion, but both can result in mitochondrial *N*-formyl peptide (mtFP) release into the circulation. However, no studies have evaluated the role of circulating mtFPs during septic shock. We found that a relatively high plasma nicotinamide adenine dinucleotide dehydrogenase subunit-6 (the most potent human mtFP) level was independently associated with the development of secondary infection in patients with septic shock and that the increased susceptibility to secondary infection is partly attributed to the suppression of polymorphonuclear leukocyte (PMN) chemotaxis by mtFP occupancy of formyl peptide receptor-1. Incorporation of these findings into therapeutic strategies may improve clinical outcomes in septic shock patients by preventing PMN chemotactic anergy.

Author contributions: W.Y.K., K.I., and C.J.H. designed research; W.Y.K., G.J.S., Y.S.J., S.M.P., S.O., S.H.K., A.R.L., J.Y.K., H.K., K.A.K., Y.K., T.K., and K.S.K. performed research; W.Y.K., K.A.K., Y.K., and B.C.K. contributed new reagents/analytic tools; W.Y.K., G.J.S., Y.S.J., S.M.P., S.O., S.H.K., A.R.L., H.K., B.C.K., T.K., K.S.K., K.I., and C.J.H. analyzed data; and W.Y.K., G.J.S., B.C.K., K.I., and C.J.H. wrote the paper.

The authors declare no competing interest.

This article is a PNAS Direct Submission. P.K. is a guest editor invited by the Editorial Board.

[1]To whom correspondence may be addressed. Email: kwy711@hanmail.net.

This article contains supporting information online at https://www.pnas.org/lookup/suppl/doi:10.1073/pnas.2018538118/-/DCSupplemental.

Published April 22, 2021.

releases elevated amounts of cytokines and chemokines into the circulation for several days even after hemodynamic stabilization (26). Because of this, chemokine gradients from blood to secondary infected sites may be diminished, but newly synthesized bacterial peptides will still be relatively concentrated in secondarily infected sites. This difference may make the role of FPR1-mediated PMN chemotaxis more important in patients with septic shock than in injured patients. However, there have been no studies evaluating the role of circulating mtFPs in patients with septic shock.

We therefore hypothesized that septic shock induces mtFP release from injured tissues or other sites into the circulation and that such released mtFPs may contribute to the development of secondary infection in patients with septic shock via suppressing FPR1-mediated PMN chemotaxis to sites of secondary infection. To study this hypothesis, we investigated whether circulating mtFP levels are independently and positively associated with the development of secondary infection in patients with septic shock who survive their early hyperinflammatory phase. We also investigated whether the increased susceptibility to secondary infection can be attributed to the suppression of PMN chemotaxis by mtFP occupancy of FPR1.

Results

Patients' Characteristics. Among 189 consecutive patients admitted to the intensive care unit (ICU) with septic shock, 180 patients provided written informed consent at admission; of these, 83 were excluded and 97 were finally enrolled (Fig. 1*A*). The 90 d mortality of enrolled patients was 36.0%. Mechanical ventilation (MV) was necessary for 39 of the 97 patients (40.2%). Central venous and urinary catheters were inserted in all patients. Central venous catheters were not routinely replaced if there were no signs of catheter insertion site infection and were removed as soon as possible when patients started enteral nutrition. Urinary catheters were replaced every 2 wk. In all of the enrolled patients, urinary catheters were maintained throughout the ICU stay. Secondary infections were identified in 15 patients. Secondary infection characteristics including isolated pathogens are shown in *SI Appendix*, Table S1. Ventilator-associated pneumonia (VAP), central line–associated bloodstream infection (CLABSI), and catheter-associated urinary tract infection (CAUTI) developed in 5, 9, and 2 patients, respectively. In one patient, VAP and CLABSI were identified simultaneously. Most secondary infections developed between 4 and 25 d after ICU admission (Fig. 1*B*). The mortality rate of patients who developed secondary infections was significantly higher than that of secondary infection–negative patients (90 d mortality 73.3% and 29.3%, respectively) ($P < 0.001$) and was particularly apparent after day 14 post-ICU admission (Fig. 1*C*).

Clinical characteristics of patients developing secondary infection and 90 d mortality are described in *SI Appendix*, Tables S2 and S3. The presence of bacteremia, blood lactate levels > 4.1 mmol/L, a duration of MV > 7 d, and the use of renal replacement therapy were significantly associated with the development of secondary infection. Furthermore, blood lactate levels > 5.5 mmol/L, sequential organ failure assessment (SOFA) scores > 9.0, a duration of MV > 4 d, and the use of renal replacement therapy were associated with increased 90 d mortality. There were no significant differences in the time to first antibiotics between secondary infection–negative patients and patients developing secondary infections (1.6 and 1.4 h, $P = 0.461$) and between 90 d survivors and nonsurvivors (1.6 and 1.7 h, $P = 0.668$).

Plasma Levels of Nicotinamide Adenine Dinucleotide Dehydrogenase Subunit-6 (ND6), Cytokines, and Chemokines. Plasma levels of ND6 (the most potent human mtFP to induce PMN chemotaxis) (12), cytokines, and chemokines at 0, 24, and 72 h are presented in Fig. 1 *D* and *E* and *SI Appendix*, Table S4. In stepwise logistic regression analysis, increases in plasma levels of ND6 at 0 h (odds ratio = 6.701, 95% CI: 1.824 to 24.618, $P = 0.004$), interleukin (IL)-6 at 24 h, IL-10 at 24 h, and growth-regulated oncogene (GRO)-α at 24 h were significantly associated with the subsequent development of secondary infection (*SI Appendix*, Table S5). Moreover, increased plasma levels of ND6 at 0 h (odds ratio = 1.660, 95% CI: 1.116 to 2.470, $P = 0.012$), IL-10 at 24 h, IL-8 at 72 h, and leukotriene B4 (LTB4) at 0 h were associated with increased 90 d mortality (*SI Appendix*, Table S5).

Effects of Circulating ND6 on Clinical Outcomes in Patients with Septic Shock. Plasma ND6 levels in patients going on to have secondary infection were higher at all time points than those in secondary infection–negative patients ($P < 0.001$) (*SI Appendix*, Fig. S1*A*). Furthermore, plasma ND6 levels in 90 d nonsurvivors were higher than those in survivors ($P = 0.015$) (*SI Appendix*, Fig. S1*B*). Plasma LTB4 levels in 90 d nonsurvivors were also higher at all time points than those in survivors ($P = 0.001$) (*SI Appendix*, Fig. S1*B*).

In multivariable analysis, a relatively high plasma ND6 level at 0 h was independently associated with both the development of secondary infection (odds ratio = 30.317, 95% CI: 2.904 to 316.407, $P = 0.004$) and increased 90 d mortality (odds ratio = 1.572, 95% CI: 1.002 to 2.465, $P = 0.049$) (*SI Appendix*, Table S6). A relatively high plasma LTB4 level at 0 h was also associated with increased 90 d mortality (odds ratio = 1.239, 95% CI: 1.003 to 1.532, $P = 0.047$) (*SI Appendix*, Table S6). Furthermore, the occurrence of secondary infection (odds ratio = 4.670, 95% CI: 1.134 to 19.230, $P = 0.033$) was independently associated with increased 90 d mortality (*SI Appendix*, Table S7).

In the receiver operating characteristic (ROC) curve analysis, the area under the curve (AUC) for the plasma ND6 level at 0 h to predict the development of secondary infection was 0.930, and its optimal cutoff value was 2,255 pg/mL (Fig. 1*F*). The AUCs for the diagnostic abilities of plasma ND6 and LTB4 at 0 h to predict 90 d mortality were 0.630 and 0.655, respectively (Fig. 1*G*).

Role of Circulating ND6 in PMN Chemotaxis in Response to Bacterial FP. To examine the role of circulating ND6 in the development of secondary infection, we first performed in vitro experiments using isolated human PMNs incubated in the control medium. In three independent experiments, the mean purity of isolated PMNs was 97.47 ± 0.42% (SD) (*SI Appendix*, Fig. S2). PMN calcium mobilization and chemotaxis in response to *N*-formyl-methionine-leucine-phenylalanine (fMLF) and ND6 were completely blocked by 10 μM cyclosporine H (CsH) (*SI Appendix*, Figs. S3 and S4).

ND6 prestimulation suppressed PMN ER calcium depletion in response to fMLF in a dose-dependent manner (Fig. 2 *A* and *B*). Furthermore, no changes were observed in the total amount of ER calcium depletion achieved with variable doses of ND6 and subsequent 100 nM fMLF (*SI Appendix*, Fig. S5). ND6 pretreatment prevented PMN chemotaxis in response to fMLF in a dose-dependent manner, same as calcium mobilization (Fig. 2*C*). ND6 pretreatment also prevented PMN chemotaxis in response to 100 nM ND6 in a dose-dependent manner (Fig. 2*D*). We saw increased nondirectional spontaneous movements (chemokinesis) of ND6- and fMLF-pretreated PMNs under the nongradient conditions (*SI Appendix*, Fig. S6 *A* and *B*). Flow cytometry showed that 10 μM CsH abolished FPR1 on the PMN membrane (Fig. 2 *E* and *F*). An addition of 100 nM fMLF significantly reduced FPR1 expression on the PMN membrane, and ND6 also reduced FPR1 expression in a dose-dependent manner (Fig. 2 *E* and *F*).

Heterologous Desensitization of CXCR2 and LTB4 Receptor (BLT1) by ND6. ND6 pretreatment suppressed PMN chemotaxis in response to 100 nM GRO-α (*SI Appendix*, Fig. S7*A*) and decreased CXCR2 expression on the PMN membrane (*SI Appendix*, Fig. S7 *B* and *C*).

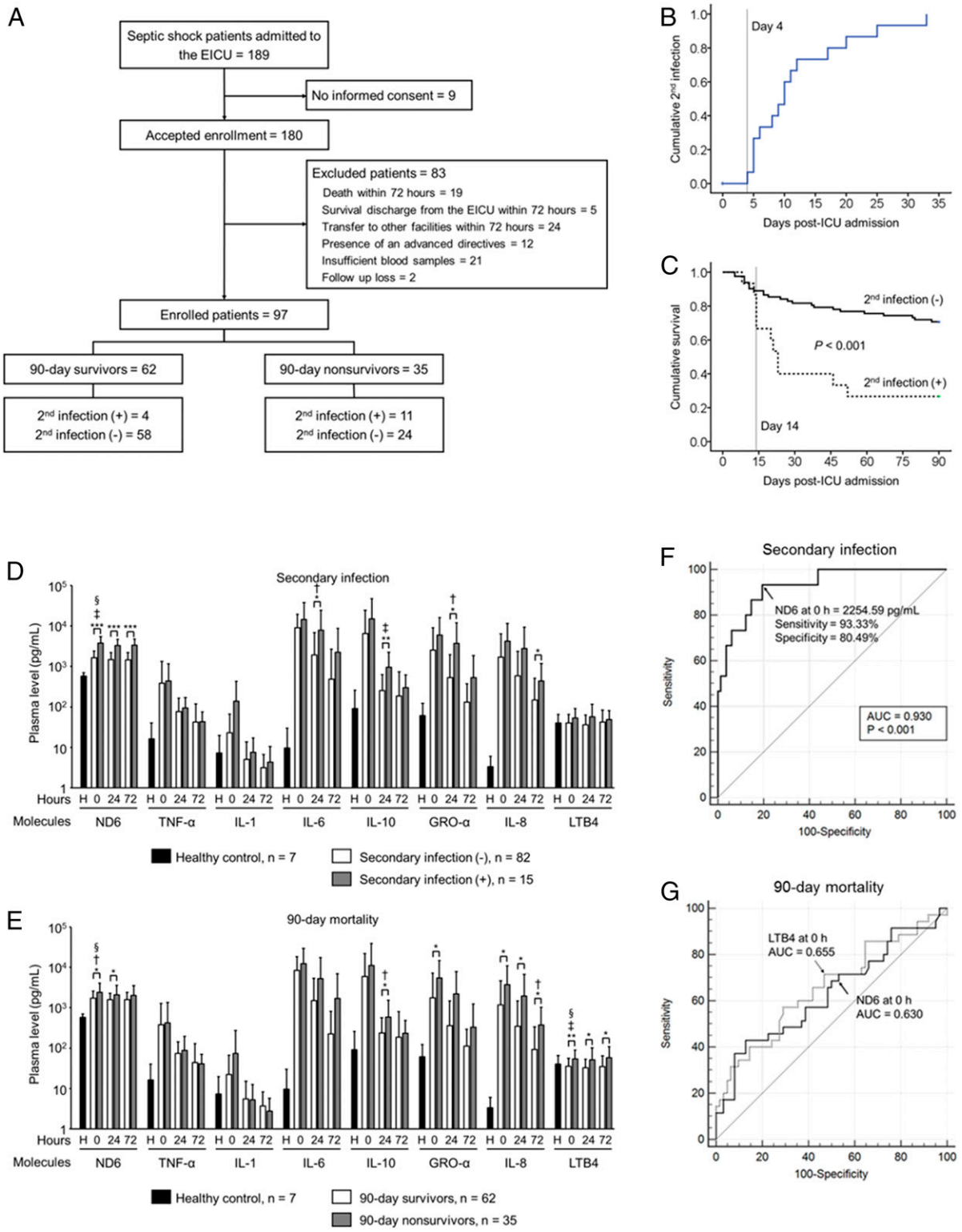

Fig. 1. Clinical data. (*A*) Enrolled patients. (*B*) Cumulative occurrence of secondary (second) infections after ICU admission. (*C*) Comparison of cumulative survival between patients going on to have secondary infections (second infection (+)) and secondary infection–negative (second infection (–)) patients. (*D*) Comparison of plasma levels of ND6, cytokines, and chemokines between second infection (+) and second infection (–) patients, and (*E*) between 90 d survivors and nonsurvivors. The data are presented as the mean ± SD. The *y* axis is expressed on a log scale. For exact values, see *SI Appendix*, Table S4. $^{*}P < 0.05$, $^{**}P < 0.01$, and $^{***}P < 0.001$ between second infection (+) and second infection (–) patients. $^{\dagger}P < 0.05$ and $^{\ddagger}P < 0.01$ in stepwise logistic regression analysis (with an entry level of 0.05 and a stay level of 0.05) (*SI Appendix*, Table S5). $^{\S}P < 0.05$ in multiple logistic regression analysis (*SI Appendix*, Table S6). (*F*) ROC curve analysis for the development of secondary infection. The AUC of the plasma ND6 levels at 0 h to predict the development of secondary infection was 0.930 ($P < 0.001$), and its optimal cutoff value was 2,255 pg/mL (the sensitivity and specificity were 93.33 and 80.49%, respectively). The cutoff value was calculated by the Youden index (*J*). (*G*) ROC curve analysis for 90 d mortality. The AUCs of the plasma ND6 levels at 0 h and LTB4 levels at 0 h to predict 90 d mortality were 0.630 ($P = 0.036$) and 0.655 ($P = 0.011$), respectively.

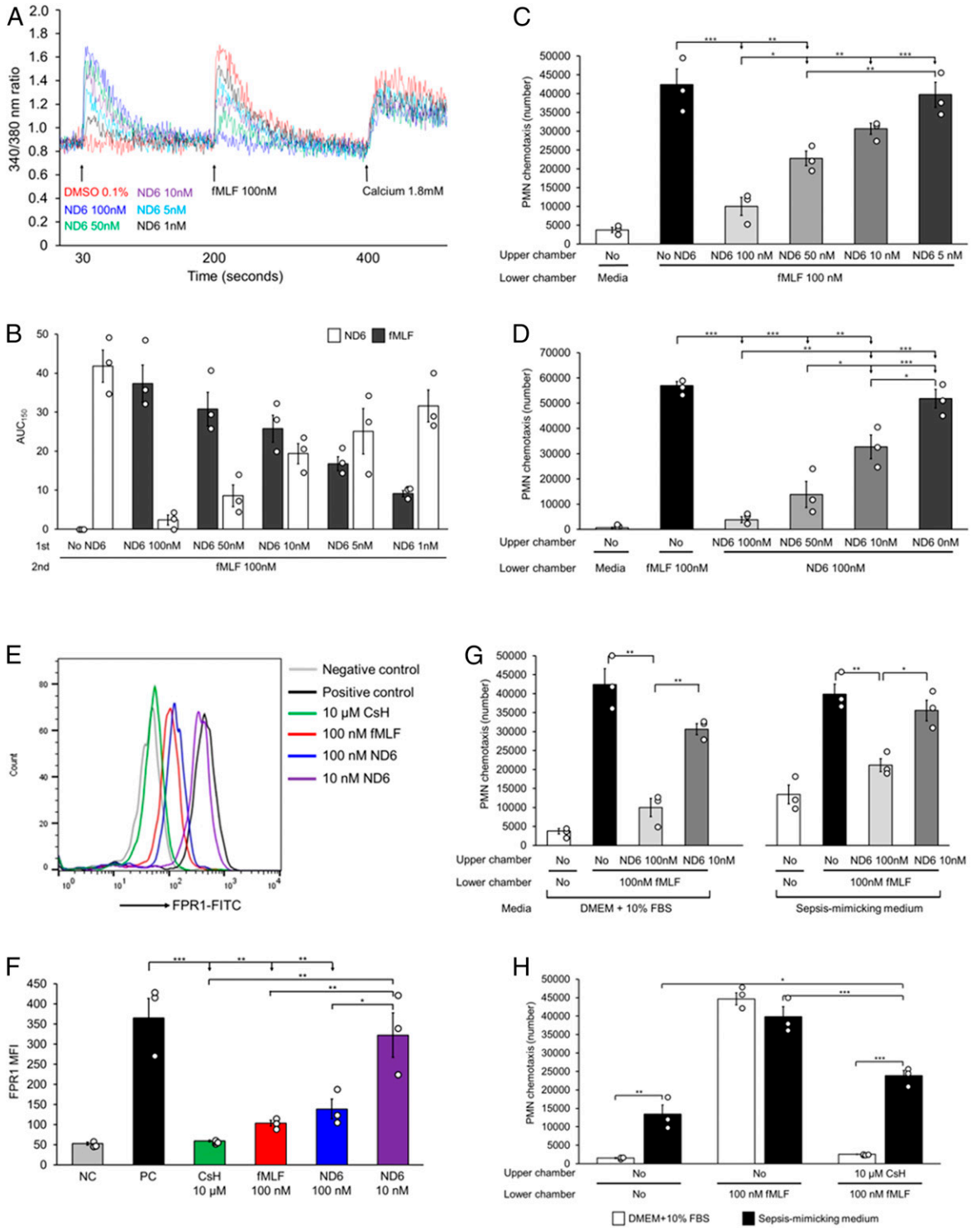

Fig. 2. Roles of ND6 in PMN chemotaxis. (*A*) ER calcium depletion in response to ND6 prestimulation and subsequent fMLF stimulation. Each line represents the mean value of each time point. (*B*) The AUCs of ER calcium depletion. The white bars represent the mean AUCs for 150 s (AUC_{150}) of ER calcium depletion in response to ND6 prestimulation, and the black bars represent the mean AUC_{150} in response to fMLF. (*C*) PMN chemotaxis in response to fMLF after ND6 pretreatment. (*D*) Gradient PMN chemotaxis in response to ND6 after ND6 pretreatment. (*E*) Representative figures of flow cytometry detecting FPR1 on the PMN membrane. (*F*) Mean fluorescence intensities of flow cytometry. The addition of 10 μM CsH completely decreased the number of FPR1 detected on the PMN membrane. Furthermore, 100 nM fMLF significantly decreased FPR1, and ND6 also decreased FPR1 in a dose-dependent manner. (*G*) Inhibitory effects of ND6 pretreatment on PMN chemotaxis in the sepsis-mimicking medium. In the sepsis-mimicking medium, PMN chemokinesis was significantly increased, and inhibitory effects of ND6 pretreatment on PMN chemotaxis in response to fMLF were weaker than in the control medium: DMEM containing 10% FBS. However, even in the sepsis-mimicking medium, 100 nM ND6 pretreatment significantly suppressed PMN chemotaxis in response to fMLF. (*H*) FPR1-blockade effects on PMN chemotaxis. In the sepsis-mimicking medium, FPR1-mediated PMN chemotaxis in response to fMLF and ND6 was significantly blocked by pretreatment with an FPR antagonist, CsH (10 μM). In the medium without fMLF or ND6, 0.1% dimethyl sulfoxide (DMSO) was added. The data are presented as the mean ± SE of three independent experiments. $*P < 0.05$; $**P < 0.01$; $***P < 0.001$.

ND6 pretreatment also suppressed PMN chemotaxis in response to 10 nM LTB4 (*SI Appendix*, Fig. S7*D*) and decreased BLT1 expression on the PMN membrane (*SI Appendix*, Fig. S7 *E* and *F*). However, FPR1 blockade by 10 μM CsH before ND6 pretreatment prevented the ND6-induced suppression of PMN chemotaxis in response to GRO-α and LTB4 as well as CXCR2 and BLT1 expression on the PMN membrane (*SI Appendix*, Fig. S7). At very high dosages, CsH may well have "off-target" effects. However, at the dose we studied here (10 μM), CsH itself did not alter PMN chemotaxis in response to GRO-α and LTB4, or CXCR2 and BLT1 expression on the PMN membrane.

FPR1-Mediated PMN Chemotaxis in Sepsis-Mimicking Medium. To simulate septic conditions, we prepared a sepsis-mimicking medium that contained a mixture of four cytokines and three chemokines at concentrations approximating those previously found in our patients with septic shock developing secondary infection, and we incubated PMNs obtained from healthy volunteers in the sepsis-mimicking medium. We investigated the effect of ND6 pretreatment on PMN chemotaxis in response to 100 nM fMLF in the sepsis-mimicking medium. Upon PMN exposure to the sepsis-mimicking medium, PMN chemokinesis significantly increased (Fig. 2*G*), and the inhibitory effects of CsH and ND6 pretreatment on PMN chemotaxis in response to fMLF were weaker than in the control medium (Fig. 2*H*). Despite these changes, ND6 pretreatment significantly suppressed FPR1-mediated PMN chemotaxis in response to fMLF, even in the presence of multiple cytokines and chemokines (Fig. 2*G*).

Microfluidic PMN Migration Chip Assay. PMN chemotactic properties, such as the fraction of completely migrated PMNs (chemotactic PMNs) among the PMNs entering microchannel entrances and their migrating velocities, were directly examined by using a microfluidic PMN migration chip (27) (*SI Appendix*, Fig. S8). Representative figures of microfluidic PMN migration chip experiments are presented in Fig. 3*A*. Images were captured at 15 min of chip-running from representative video files (Movie S1). Similar to the results of PMN chemotaxis tested in the conventional pore-membrane plate (*SI Appendix*, Fig. S6*A*), PMN chemokinesis increased when PMNs were exposed to 100 nM ND6 and/or the sepsis-mimicking medium (Fig. 3 *B* and *C*). When chemokinetic PMNs were subtracted, ND6 pretreatment significantly reduced the fraction of chemotactic PMNs in response to fMLF by 80.4% in the control medium and 88.1% in the sepsis-mimicking medium (Fig. 3*D*). In contrast, ND6 pretreatment increased the migrating velocities of PMNs in the control medium but not in the sepsis-mimicking medium (Fig. 3*E*). Although the difference was not significant, overall chemotactic responses were decreased in sepsis-mimicking versus control media.

Effects of ND6 on Bacteria-Killing Activities of PMNs. In PMNs incubated with *Staphylococcus aureus* (Fig. 4 *A* and *B*) and *Escherichia coli* (Fig. 4 *C* and *D*), ND6 treatment slightly reduced bacteria-killing activities of PMNs. However, there were no statistical significances.

Peripheral Blood Mononuclear Cell–Bacteria Conditioned Medium. After 24 h incubation of peripheral blood mononuclear cell (PBMC) with *S. aureus* or *E.coli*, ND6 levels in the PBMC–bacteria conditioned medium increased. However, in bacteria-only conditioned medium and in media containing sonicated bacteria, ND6 levels did not increase (*SI Appendix*, Fig. S9). ND6 has not been reported to occur in bacteria, but to confirm, we performed this experiment. These data indicate that human mtFPs were not released from bacteria but from the human PBMCs. Our recent study also showed that monocytes stimulated by infectious stimuli actively released mtDAMPs into the circulation via microparticles (28).

Plasma of Patients with Septic Shock Who Developed Secondary Infections. To verify the direct correlation between circulating ND6 and the development of secondary infection, we performed ex vivo experiments with prospectively collected plasma samples and isolated PMNs from patients with septic shock who had developed secondary infections ($n = 3$) and secondary infection–negative patients ($n = 3$) between 10 and 18 d after ICU admission. Clinical characteristics of enrolled patients for this ex vivo study and their plasma levels of ND6, cytokines, and chemokines are shown in *SI Appendix*, Table S8. At the onset of secondary infection, plasma ND6 levels in patients with septic shock who developed secondary infections (2,521 pg/mL) were higher than plasma ND6 levels in healthy volunteers (627 pg/mL) and secondary infection–negative patients (951 pg/mL) (Fig. 5*A*). Plasma mtDNA levels in patients who developed secondary infections (2,054 pg/mL) were also higher than in healthy volunteers by (14 pg/mL) and secondary infection–negative patients (143 pg/mL) (Fig. 5*B*). However, plasma LTB4 levels at the onset of secondary infection were significantly lower in patients who developed secondary infections (65 pg/mL) than in secondary infection–negative patients (82 pg/mL), unlike plasma LTB4 levels during the early 72 h period of septic shock (Fig. 5*C*).

When PMNs obtained from healthy volunteers were exposed to the plasma of patients with septic shock who developed secondary infections, PMN chemotaxis in response to 100 nM fMLF significantly decreased, when compared to PMNs exposed to the plasma of healthy volunteers ($P < 0.001$) and secondary infection–negative patients ($P = 0.001$) (Fig. 5*D*). Furthermore, FPR1 expression detected on the PMN membrane in PMNs exposed to the plasma of patients who developed secondary infections also decreased compared to PMNs exposed to the plasma of healthy volunteers ($P = 0.018$) and secondary infection–negative patients ($P = 0.030$) (Fig. 5 *E* and *F*).

Previous studies have reported that CD16 expression is modulated during sepsis-induced immunosuppression (29). In the present study, PMNs gated by forward versus side scatter (FSC versus SSC) and gated by CD16-positive among whole cells exposed to the plasma of healthy volunteers were 61.6 and 67.5%, respectively. PMNs gated by FSC versus SSC and by CD16-positive among whole cells exposed to the plasma of patients who developed secondary infections were 68.7 and 72.3%, respectively (*SI Appendix*, Fig. S10). Even in the plasma of patients who developed secondary infections, the number of PMNs gated by CD16-positive did not substantially differ from the number of PMNs gated by FSC versus SSC. Thus, we gated PMNs by CD16-positively.

PMNs in Patients with Septic Shock Who Developed Secondary Infections. Next, we directly examined the chemotactic response to 100 nM fMLF in PMNs obtained from healthy volunteers, patients with septic shock who had developed secondary infections, and secondary infection–negative patients. PMNs from patients who developed secondary infections exhibited a significantly lower chemotactic response than PMNs from healthy volunteers ($P = 0.008$) and secondary infection–negative patients ($P = 0.005$) (Fig. 5*G*). FPR1 expression on the PMN membrane in PMNs from patients who developed secondary infections also decreased compared to PMNs from healthy volunteers ($P = 0.025$) (Fig. 5 *H* and *I*).

Discussion

The present study shows that plasma ND6 levels are elevated in patients with septic shock compared to healthy volunteers. Moreover, high plasma ND6 levels on admission are strongly associated with the development of secondary infection and increased 90 d mortality in patients with septic shock admitted to the ICU for longer than 72 h. The occurrence of secondary infection was independently associated with increased 90 d mortality.

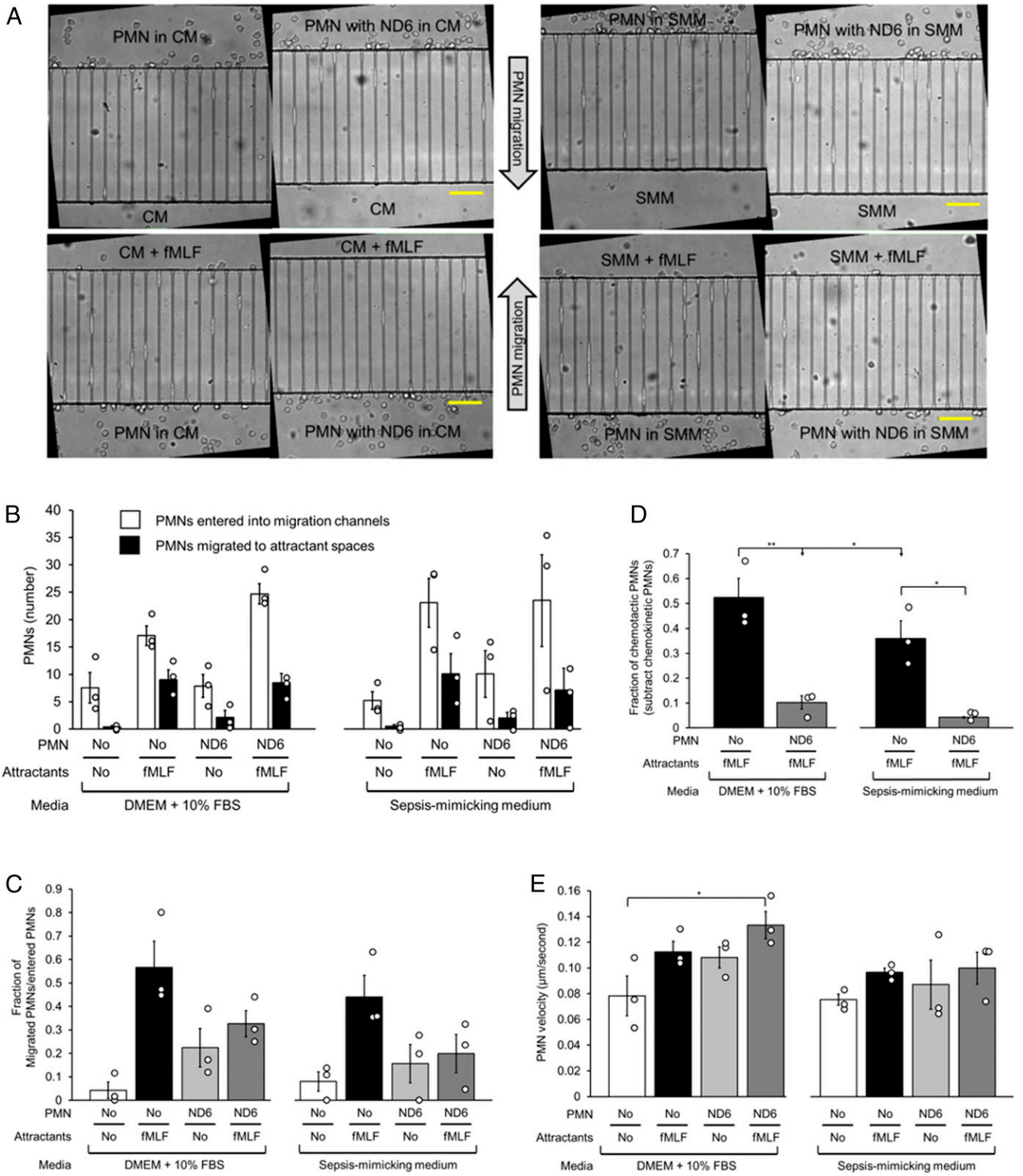

Fig. 3. Microfluidic PMN migration chip assay. (*A*) Representative figures of microfluidic PMN migration chip experiments. Images were captured at 15 min of chip running from Movie S1 (scale bar, 50 μm length). (*B*) The number of completely migrated PMNs (chemotactic PMNs) and PMNs entering microchannel entrances in the control medium (CM, DMEM containing 10% FBS) and the sepsis-mimicking medium (SMM). (*C*) The fraction of chemotactic PMNs among the PMNs entering microchannel entrances. (*D*) Inhibitory effects of 100 nM ND6 pretreatment on PMN chemotaxis after subtracting chemokinetic PMNs. ND6 pretreatment significantly reduced the fraction of chemotactic PMNs in response to fMLF in both the CM and SMM. Representative figures of chemotactic and chemokinetic PMN movements are shown in *SI Appendix*, Fig. S13 *A* and *B*, respectively. (*E*) The migrating velocities (μm/second) of PMNs. ND6 pretreatment increased the velocities of PMNs in the CM but not in the SMM. The data are presented as the mean ± SE of three independent experiments. Four different conditions were studied in each experiment, and PMN movements were observed in five fields at random in each chip. $*P < 0.05$; $**P < 0.01$; $***P < 0.001$.

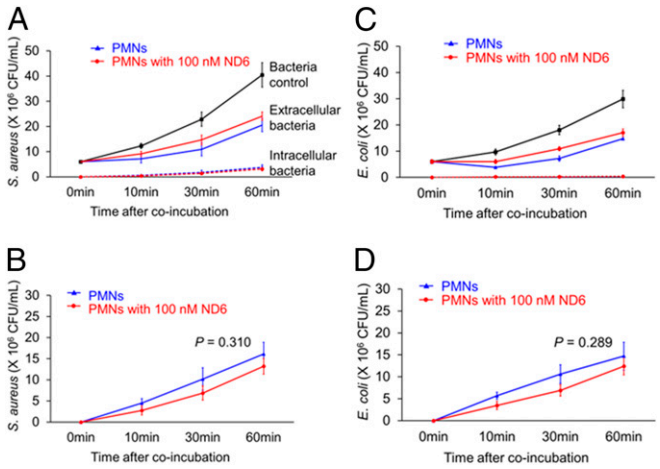

Fig. 4. Effects of ND6 pretreatment on bacteria-killing activities of PMNs. (*A*) Changes in the number of CFUs of *S. aureus* during the 60 min incubation period with PMNs. Each line represents the mean value of each time point. (*B*) Calculated *S. aureus* killing activities of untreated and 100 nM ND6-treated PMNs. Bactericidal activity was calculated by subtracting the number of CFUs of extracellular bacteria and intracellular bacteria in bacteria with PMNs from the number of CFUs of extracellular bacteria in bacteria-only control. (*C*) Changes in the number of CFUs of *E. coli* during the 60 min-incubation period with PMNs. (*D*) Calculated *E. coli* killing activities of untreated and 100 nM ND6-treated PMNs. ND6 treatment slightly suppressed the bactericidal activity of PMNs both in the PMNs incubated with *S. aureus* and *E. coli*, but the difference was not significant. The data are presented as the mean ± SE of three independent experiments.

Before day 14 post-ICU admission, the mortality rate of patients who developed secondary infections was not different from that of secondary infection–negative patients. However, increased mortality after day 14 was significantly associated with the occurrence of secondary infection. These data suggest that an increase in the circulating ND6 level during the early period of septic shock may contribute to the development of secondary infection and contributing to an increase in delayed mortality in patients with septic shock who survived their early hyperinflammatory phase. Furthermore, the high diagnostic ability of plasma ND6 levels is not inferior to conventional biomarkers, indicating that circulating ND6 may be used as a potential prognostic biomarker in patients with septic shock (30).

To examine the potential importance of circulating ND6 in the development of secondary infection in patients with septic shock, we performed in vitro experiments using isolated human PMNs. For the purpose of these experiments, we hypothesized that during septic shock, cytokines and chemokines are evenly distributed in the circulation but that a significant gradient in bacterial FPs is likely to exist between secondary infected sites and the circulation, which derives PMN recruitment. Thus, to simulate septic conditions, we made a sepsis-mimicking medium that contained a mixture of four cytokines and three chemokines based on our patient plasma study results. Moreover, to simulate secondary infected sites, fMLF, a canonical bacterial FP, was added to the sepsis-mimicking medium. We found differences in PMN chemotactic responses in sepsis-mimicking versus control media. Upon PMN exposure to the sepsis-mimicking medium, PMN chemokinesis increased, as was found in the literature (31), and the proportion of FPR1-mediated chemotaxis in response to bacterial FP decreased compared to the control medium. These data suggest that non-mtFP-FPR1–mediated pathways, such as GPCR modulation by other cytokines and chemokines and/or unknown mediator-induced FPR1 down-regulation, are also involved in PMN chemotaxis during septic shock (32, 33).

We also examined the chemotactic properties of PMNs using a microfluidic PMN migration chip. This system potentially minimizes the gravitational interference that may contribute to chemokinetic transport of PMNs or cellular debris down the transwell, as may occur in conventional chemotaxis experiments (34, 35). Although no significant differences were observed, in the sepsis-mimicking medium, the fraction of chemotactic PMNs and their migrating velocity appeared to be reduced compared to those in the control medium. These findings might be partly due to heterologous desensitization of other GPCRs by mtFP occupancy of FPR1 (11) (*SI Appendix*, Fig. S7). Despite these differences, ND6 pretreatment significantly suppressed FPR1-mediated PMN chemotaxis in response to bacterial FP in the sepsis-mimicking medium as it did in the control medium.

Next, we found that ND6 treatment appeared to reduce the bacteria-killing activities of PMNs, though the effect was not significant. These data indicate that the increased susceptibility to secondary infection is probably due to the suppression of FPR1-mediated PMN chemotaxis to secondary infected sites rather than a loss of PMN bactericidal activity.

Finally, we studied plasma samples and PMNs obtained from patients with septic shock who had developed secondary infections and secondary infection–negative patients. At the onset of secondary infection, plasma ND6 levels in patients who developed secondary infections were significantly higher than in secondary infection–negative patients, as shown during the early 72 h period of septic shock. Plasma mtDNA levels were also higher in patients who developed secondary infections than in secondary infection–negative patients. We have previously shown a subset of 5/13 human mtFPs act similarly (11, 12). ND6 is likely to be both the most potent FPR1 agonist and a marker for the other mtFPs. However, other mtDAMPs like mtDNA released during septic shock may act differently, such as modulating toll-like receptor-9–related pathways (28). The SOFA scores at the onset of secondary infection were significantly higher in patients who developed secondary infections (10.7 ± 1.5) than in secondary infection–negative patients (4.3 ± 1.2) (*SI Appendix*, Table S8). Consistently high circulating mtFP levels might be attributed to ongoing tissue injuries. Furthermore, active mtDAMP release via microparticle extrusion from monocytes stimulated by secondarily infected bacteria might also increase circulating mtFP levels (28). Exposure to the plasma of patients who developed secondary infections, that contained large amounts of ND6, significantly suppressed the chemotaxis of PMNs obtained from healthy volunteers and FPR1 expression on the PMN membrane. When we directly studied PMNs obtained from patients who developed secondary infections, PMN chemotaxis in response to bacterial FP and FPR1 expression on the PMN membrane significantly decreased compared to PMNs from healthy volunteers and secondary infection–negative patients.

Unlike during the early period of septic shock, at the onset of secondary infection, plasma LTB4 levels in patients with septic shock who developed secondary infections were significantly lower than in secondary infection–negative patients. Previous experimental studies reported that LTB4 might be a relay signal to enhance FPR1-mediated PMN chemotaxis (36). These results suggest the possible important role of LTB4 in developing secondary infection due to immune paralysis in patients recovering from septic shock.

Our findings may indeed point to the importance of high circulating mtFP levels that persists while other inflammatory mediators subside. This may suggest the crucial role of mtDAMPs in the worsening of clinical outcomes in patients recovering from septic shock. Therefore, we suggest that immunotherapy desensitizing and/or eliminating circulating mtFPs, before secondary infection can occur, may be a therapeutic strategy to reduce the development of secondary infection and delayed mortality in patients with septic shock whose plasma ND6 levels at admission are equal or greater

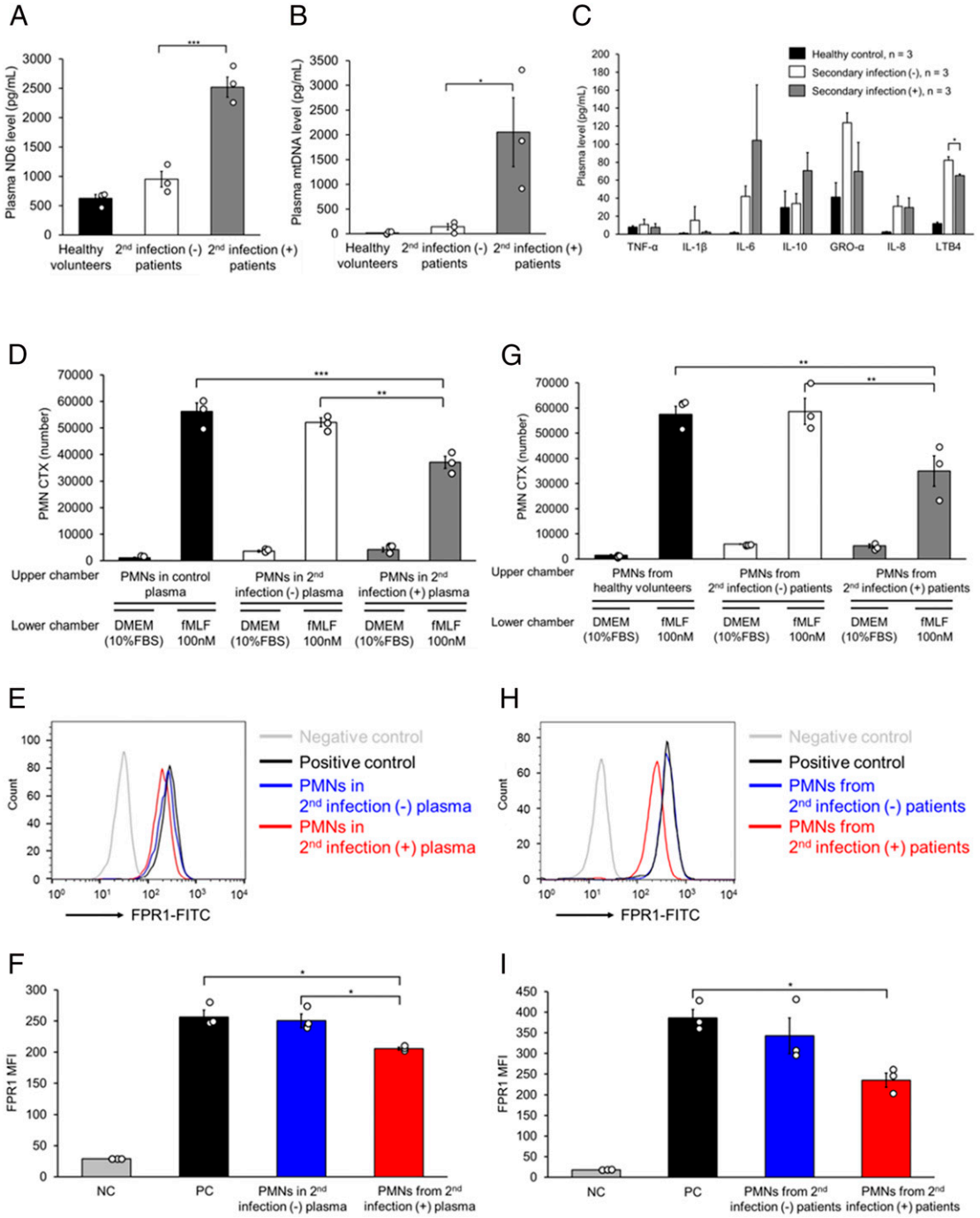

Fig. 5. Plasma and PMNs of patients with septic shock at the onset of secondary infection. (*A*) Plasma ND6 levels of the plasma obtained from patients who had developed secondary infections (second infection (+), $n = 3$) and secondary infection–negative patients (second infection (–), $n = 3$). (*B*) mtDNA levels. (*C*) Plasma levels of cytokines and chemokines. Each sample was assayed in duplicate. At the onset of secondary infection, plasma ND6 levels in second infection (+) patients (2,521 pg/mL) were still higher than plasma ND6 levels in healthy volunteers (627 pg/mL) and second infection (–) patients (951 pg/mL). Plasma mtDNA levels in second infection (+) patients (2,054 pg/mL) were also higher than in healthy volunteers (14 pg/mL) and second infection (–) patients (143 pg/mL). However, plasma LTB4 levels at the onset of secondary infection were significantly lower in second infection (+) patients (65 pg/mL) than in second infection (–) patients (82 pg/mL), unlike plasma LTB4 levels during the early 72 h period of septic shock. For detailed information, see *SI Appendix*, Table S8. (*D*) The chemotaxis of PMNs obtained from healthy volunteers exposed to the plasma of second infection (+) and second infection (–) patients. When PMNs obtained from healthy volunteers were exposed to the plasma of second infection (+) patients, PMN chemotaxis in response to 100 nM fMLF significantly decreased, when compared to PMNs exposed to the plasma of second infection (–) patients ($P = 0.001$). (*E*) Representative figures of flow cytometry detecting FPR1 on the PMN membrane and (*F*) Mean fluorescence intensities. FPR1 expression on the PMN membrane in PMNs exposed to the plasma of second infection (+) patients also decreased compared to PMNs exposed to the plasma of second infection (–) patients ($P = 0.030$). (*G*) The chemotaxis of PMNs obtained from second infection (+) and second infection (–) patients in response to 100 nM fMLF. The chemotaxis of PMNs from second infection (+) patients significantly decreased, when compared to PMNs from second infection (–) patients ($P = 0.005$). (*H*) Representative figures of flow cytometry detecting FPR1 on the PMN membrane and (*I*) Mean fluorescence intensities. FPR1 expression on the PMN membrane in PMNs from second infection (+) patients also decreased compared to PMNs obtained from healthy volunteers ($P = 0.030$), but FPR1 expression of the PMN membrane in PMNs from second infection (–) patients did not decrease significantly. The data are presented as the mean ± SE of three independent experiments. $*P < 0.05$; $**P < 0.01$; $***P < 0.001$.

than 2,255 pg/mL (Fig. 1*F*). Five highly potent mtFPs, including ND6, ND3, ND4, ND5, and cytochrome *c* oxidase subunit 1 (Cox1), might be candidates for this immunotherapy (12). This immunotherapy may preserve FPR1-mediated PMN chemotaxis in response to bacterial FPs, which is more concentrated in secondary infected sites, in the presence of circulating chemokines.

The present study has several limitations. First, the septic shock population studied may not be representative of all patients with sepsis or even all patients with septic shock. In order to investigate the role of mtFPs in septic shock, we only enrolled patients who survived their early hyperinflammation phase and thus were admitted to the ICU for longer than 72 h. Thus, unlike other studies (37, 38), the plasma concentrations of many mediators (with the notable exception of LTB4) were not independently associated with 90 d mortality. Second, our in vitro experiments used a model system where we used fMLF and a sepsis-mimicking medium to simulate secondary infected sites during septic shock. We made this system to perform in vitro experiments under the well-controlled environments mimicking septic shock patients' plasma. Although this system may not reflect all clinical circumstances equally, it is based on real clinical data, and we therefore believe it to be clinically relevant. Following ex vivo study, results support the clinical relevance of this system. Third, this study investigated only changes in bacteria-killing activities of PMNs induced by ND6 treatment. When a bacterial infection occurs, PMNs kill bacteria by phagocytosis, intracellular killing, and extracellular traps (39). We did not investigate these individual steps, but we found that the overall bactericidal activity of PMNs was not significantly affected by ND6. Fourth, during septic shock, the phenotypes and functions of immune cells may also be altered (29, 40, 41). Particularly, macrophage, dendritic cells, and monocytes also express membrane FPR1 (42). To more fully understand the role of circulating mtFPs in septic shock, the remaining questions should be answered by conducting further research using freshly collected immune cells and plasma samples from patients with septic shock treated with or without anti-mtFP antibodies.

Conclusions

In the present study, we found that an increase in circulating mtFPs appeared to contribute to the development of secondary infection and increased delayed mortality in patients with septic shock who survived their early hyperinflammatory phase. We also found that the increased susceptibility to secondary infection was at least in part mediated by the suppression of FPR1-mediated PMN chemotaxis to secondary infected sites. Incorporation of these findings into therapeutic strategies may improve clinical outcomes in patients with septic shock by preventing PMN chemotactic anergy.

Materials and Methods

Please see *SI Appendix* for a detailed version of all materials and methods.

Patients. The present clinical study was a retrospective observational study that used prospectively collected clinical data and plasma samples. The repository of clinical data and blood samples from patients with septic shock, the repository of blood samples from healthy volunteers, and the use of stored samples were approved by the Institutional Review Board of Seoul National University College of Medicine/Seoul National University Hospital (IRB number: 1707-012-865, 1806-125-954, and 1904-033-1024, respectively). Written informed consent was obtained from each patient or legally authorized representative and each healthy volunteer. We enrolled consecutive patients with septic shock admitted from the emergency department to our ICU between February 2016 and January 2019. Exclusion criteria included no informed consent, age < 18 y old, death or survival discharge from the ICU within 72 h post-ICU admission (43), transfer to another facility within 72 h, presence of an advanced directive to withhold or withdraw life-sustaining treatment, insufficient blood samples, and follow-up loss.

We screened sepsis patients with the criteria of the quick SOFA score ≥2 (44). We infused crystalloid (30 mg/kg), obtained blood cultures, and attempted to administer intravenous broad-spectrum antibiotics within 1 h. Next, we calculated the SOFA score. If the SOFA score was ≥2, mean arterial pressure was <65 mmHg after hydration, and serum lactate level was >2 mmol/L, the patient was diagnosed with septic shock (44). These patients with septic shock were admitted to the ICU as soon as possible. After admission to the ICU, we collected demographic and laboratory data. Blood samples were obtained from patients at 0, 24, and 72 h after ICU admission through an arterial catheter. The repository protocol for patients with septic shock is registered at ClinicalTrials.gov (NCT01670383).

The primary outcome was the development of secondary infection–like VAP, CLABSI, and CAUTI (*SI Appendix*, Table S9) (45). The secondary outcome was 90 d mortality.

Plasma Levels of Cytokines and Chemokines. Plasma levels of tumor necrosis factor-α (TNF-α), IL-1β, IL-6, IL-8, IL-10, and GRO-α were measured with a Luminex bead assay using the Human XL Cytokine Discovery Panel (LKTM014, R&D Systems). Plasma LTB4 levels were measured by enzyme-linked immunosorbent (ELISA) assay using the LTB4 Parameter Assay Kit (KGE006B, R&D Systems). Each sample was assayed in duplicate.

MtFPs. Among 13 human mtFPs, the most potent stimulator of ER calcium depletion and PMN chemotaxis was ND6 followed by ND3, ND4, ND5, and Cox1 (12). Therefore, in this study, we measured plasma ND6 levels using the human NADH-ubiquinone oxidoreductase chain 6 ELISA kit (MBS936598, MyBioSource). Each sample was assayed in duplicate. For in vitro experiments, ND6 hexapeptides (*N*-formyl-methionine-methionine-tyrosine-alanine-leucine-phenylalanine, *N*-formyl-MMYALF) were synthesized by Peptron.

Human PMN Isolation. Human PMNs and PBMCs were isolated from freshly drawn healthy volunteer blood (11, 12). With the permission of the Institutional Review Board (IRB) of Seoul National University College of Medicine/Seoul National University Hospital (IRB number: 1605-044-760), we received written informed consent from healthy volunteers and obtained fresh blood from them for in vitro and ex vivo experiments.

The purity of isolated human PMNs was determined by flow cytometry using a BD FACSCalibur (BD Biosciences). In brief, human leukocytes were sorted by using a fluorescein (FITC)-conjugated anti-human CD15 antibody (301903, BioLegend). Among these cells, CD49d-negative CD16-positive cells detected with a phycoerythrin/cyanine 7 (PE/Cy7)-conjugated anti-human CD49d antibody (304313, BioLegend) and an allophycocyanin (APC)-conjugated anti-human CD16 antibody (360705, BioLegend) were counted as PMNs.

PMN Calcium Mobilization. PMNs were loaded with fura2-AM (F1221, Thermo Fisher) for 45 min at 37 °C, and fluorescence was measured by using a spectrofluorometer (FluoroMax Plus-C, Horiba, Ltd) at 505 nm with 340/380 nm dual-wavelength excitations at 37 °C (12). ER calcium depletion was assessed by measuring the 340 nm/380 nm ratio and was quantified as the AUCs for 150 s (AUC_{150}). The role of FPR1 in calcium mobilization was determined by pretreatment with an FPR antagonist, CsH (10μM, SML1575, Sigma-Aldrich) (42, 46). The most potent concentration of fMLF for FPR1 stimulation was 100 nM fMLF (*SI Appendix*, Fig. S11*A*), and 10 μM CsH completely blocked the FPR1-stimulating effects of fMLF (*SI Appendix*, Fig. S11*B*). Three independent experiments were performed.

PMN Chemotaxis. To assess PMN chemotaxis, a multiScreen 96-well plate with a 3 μm pore membrane (MAMIC3S10, Merck Millipore) was used as previously described (11, 12, 47, 48). PMNs were resuspended in the control medium, namely, Dulbecco's modified Eagle's medium (DMEM, 11885-084, Thermo Fisher) containing 10% fetal bovine serum (FBS, F2442, Sigma-Aldrich) and incubated for 45 min at 24 °C with ND6 (0, 5, 10, 50, or 100 nM) or fMLF (100 nM). To determine the role of FPR1, PMNs were pretreated with 10 μM CsH for 15 min at 24 °C before treatment. PMNs were placed in the plate's upper chambers (0.1×10^6 cells in 75 μL per well). DMEM containing 10% FBS supplemented with 100 nM fMLF, 100 nM ND6, GRO-α (100 nM, 78063, STEMCELL Tech. Inc.), or LTB4 (10 nM, L0517, Sigma-Aldrich) (150 μL per well) was placed in the lower chambers. The plate was incubated for 60 min in an incubator at 37 °C with 5% carbon dioxide (CO_2). Three independent experiments were performed in quadruplicate.

Receptor Expression on the PMN Membrane. Receptor expression on the PMN membrane was detected by flow cytometry using BD FACSCalibur (BD Biosciences). An FITC-conjugated anti-human FPR1 antibody (FAB3744F, R&D

Systems) was used to detect FPR1 on the PMN membrane. FITC-conjugated anti-human CXCR2 (551126, BD Biosciences) and PE-conjugated anti-human BLT1 (LS-C16203-100, LifeSpan Biosciences Inc.) antibodies were applied to detect CXCR2 and LTB4 receptor (BLT1) on the PMN membrane. An APC-conjugated anti-human CD16 antibody (360705, BioLegend) was used for PMN isolation. Three independent experiments were performed.

Sepsis-Mimicking Medium. To simulate septic conditions, we made a sepsis-mimicking medium that contained a mixture of four cytokines and three chemokines at concentrations approximating those previously found in our patients with septic shock with secondary infection: human recombinant TNF-α (25 pM, PHC3015, Thermo Fisher), IL-1β (10 pM, PHC0814, Thermo Fisher), IL-6 (0.7 nM, PHC0065, Thermo Fisher), IL-8 (0.5 nM, I1645, Sigma-Aldrich), IL-10 (0.7 nM, MBS142362, MyBiosource), GRO-α (0.75 nM, 78063, STEMCELL Tech. Inc.), and LTB4 (0.15 nM, L0517, Sigma-Aldrich) in DMEM containing 10% FBS.

Microfluidic PMN Migration Chip Assay. We fabricated a microfluidic PMN migration chip by standard photolithography as described (27). Briefly, three parallel wide chambers with a width of 200 μm and a height of 50 μm and multiple narrow connecting microstructures with a width of 3 μm, a height of 3 μm, and a length of 200 μm were created on a silicon wafer by photolithography. The patterns were then transferred to a polydimethylsiloxane (PDMS) slab, resulting in PDMS microchannels (*SI Appendix*, Fig. S8*A*). A culture medium with an attractant flowed into the attractant chamber, and culture medium without an attractant flowed to the control chamber simultaneously, forming a diffusion-driven chemotactic gradient across the narrow connecting microchannels (*SI Appendix*, Fig. S12).

Four different conditions were studied (*SI Appendix*, Fig. S8*B*). During the 30 min of chip running, PMN movements in each condition were recorded. PMNs entering and penetrating microchannels, observed in five fields at random in each chip, were discriminated and counted manually. Next, the fraction of completely migrated PMNs to the attractant spaces (chemotactic PMNs) among the PMNs entering microchannel entrances was calculated. The migrating velocities of PMNs were measured by using ImageJ software with the MTrackJ plugin. Migrated PMNs into the control medium or sepsis-mimicking medium without fMLF were considered chemokinetic PMNs (PMNs with nondirectional spontaneous movements). Representative images of chemotactic and chemokinetic PMN movements are shown in *SI Appendix*, Fig. S13 *A* and *B*, respectively. Three independent experiments were performed.

Bacteria-Killing Activities of PMNs. Effects of ND6 treatment on PMN bactericidal activity were estimated as previously described (49). *S. aureus* (14458) and *E. coli* (35401) were purchased from American Type Culture Collection. In brief, 5.0×10^6 of *S. aureus* and *E.coli* were opsonized in 2 mL of supplemented phosphate-buffered saline (sPBS) containing 10 mM sodium phosphate buffer (pH 7.4), 140 mM NaCl, 1 mM $CaCl_2$, 0.5 mM $MgCl_2$, and 5.6 mM glucose for 20 min in a 10 rpm rotator at 37 °C. Next, bacteria were mixed with the same volume of sPBS containing 10% serum (bacteria-growth control), 5.0×10^6 PMNs with 0.1% dimethyl sulfoxide (DMSO) (bacteria with no-treated PMNs), and 5.0×10^6 PMNs with 100 nM ND6 (bacteria with ND6-treated PMNs) and incubated for 60 min in a 10 rpm rotator at 37 °C.

At 0, 10, 30, and 60 min, bacteria-killing activities were calculated by subtracting colony forming units (CFUs) of extracellular bacteria and intracellular bacteria in bacteria with PMNs from CFUs of extracellular bacteria in bacteria only. Then, we compared the bactericidal activities of untreated PMNs and ND6-treated PMNs. Three independent experiments were performed in triplicate.

Plasma and PMNs of Patients with Septic Shock at the Onset of Secondary Infection. For ex vivo experiments, we prospectively collected blood samples from patients with septic shock who had developed secondary infections ($n = 3$) and secondary infection–negative patients ($n = 3$) between 10 and 18 d after ICU admission. With the updated permission of the IRB of Seoul National University College of Medicine/Seoul National University Hospital (IRB number: 1605-044-760), we received renewed written informed consent from patients with septic shock or their legally authorized representatives.

Using PMNs obtained from healthy volunteers, we studied changes in PMN chemotaxis toward 100 nM fMLF and FPR1 expression on the PMN membrane, after a 45 min exposure to the plasma of patients with septic shock who developed secondary infections or to the plasma of secondary infection–negative patients. Next, by using PMNs obtained from patients with septic shock, we directly compared PMN chemotaxis in response to fMLF and FPR1 expression on the PMN membrane between secondary infection–positive and secondary infection–negative patients.

Plasma mtDNA Levels. Quantitative real-time PCR was performed to detect and quantify mtDNA in the plasma as previously described (14). Primers for human cytochrome B (forward 5″-ATGACCCCAATACGCAAAAT-3″ and reverse 5″-CGAAGTTTCATCATGCGGAG-3″) were synthesized by Bioneer Corp.

PBMC–Bacteria Conditioned Medium. We incubated 2.5×10^6 of PBMC with 2.5×10^6 CFU of *S. aureus* or *E. coli* in DMEM containing 10% FBS for 24 h at 37 °C with 5% CO_2. PBMC alone and bacteria alone were also incubated. After centrifugation at 20,000 *g* for 10 min at 4 °C, supernatants were collected (PBMC-bacteria conditioned medium). Next, bacteria-alone pellets were resuspended, sonicated 10 times for 30 s each, and centrifuged again. The supernatants were collected, and ND6 levels were measured. Four independent experiments were performed in duplicate.

Statistics. In the present study, the 90 d mortality rate of patients who developed secondary infections and secondary infection–negative patients were 73.3 and 29.3%, respectively, and a sample size of equal or greater than 12 per group showed a power of 0.8 and a significance level of 0.05. Cumulative survival and the cumulative occurrence of secondary infection were analyzed using Kaplan–Meier survival analysis with the log-rank post hoc test. Clinical demographic and laboratory data were analyzed by using the Student's *t* test or χ^2 test. Differences in parameters for 72 h between patients developing secondary infection and secondary infection–negative patients and between 90 d survivors and nonsurvivors were analyzed using the repeated measures ANOVA. Serial data were analyzed using stepwise logistic regression analysis (with an entry level of 0.05 and a stay level of 0.05). Next, to determine which parameters were independently associated with clinical outcomes in patients with septic shock, multiple logistic regression analysis was applied. The diagnostic abilities of ND6 for the development of secondary infection and increased 90-d mortality were evaluated by calculating the AUCs in the ROC curve analysis, and the cutoff value was calculated by the Youden index (*J*). *P* values less than 0.05 were considered statistically significant, and the significance levels quoted are two-sided. In vitro and ex *vivo* experimental data were analyzed using the one-way analysis of variance with Tukey's post hoc test. Bacteria killing activities of PMNs were analyzed using the repeated-measures analysis of variance test. These statistical analyses were conducted by using IBM SPSS version 23.0 for Windows (SPSS).

Data Availability. All study data are included in the article and/or supporting information.

ACKNOWLEDGMENTS. This study was mainly supported by National Research Foundation of Korea (NRF) grant funded by the Korean government Ministry of Education, Science and Technology (MEST) (Grant 2019R1A2C1005119 to W.Y.K.). This study was supported, in part, by Congressionally Directed Medical Research Programs award funded by US Department of Defense (Grant W81XWH-16-1-0464 to C.J.H.) and by NRF grant funded by the Korean government (MEST) (Grant 2017R1D1A1B03035443 to B.C.K.). The repository of clinical data and blood samples from septic shock patients was supported by Seoul National University Hospital Research Fund (Grant 25-2016-0040 to G.J.S.), and the human biospecimens were stored in and were provided by our Hospital Human Biobank, a member of the National Biobank of Korea, supported by the Ministry of Health and Welfare. We acknowledge and greatly appreciate the patients who agreed to participate in this study. We are also grateful to the individuals who volunteered for this study.

1. L. A. van Vught *et al*.; MARS Consortium, Incidence, risk factors, and attributable mortality of secondary infections in the intensive care unit after admission for sepsis. *JAMA* **315**, 1469–1479 (2016).
2. G. J. Zhao *et al*., Incidence, risk factors and impact on outcomes of secondary infection in patients with septic shock: An 8-year retrospective study. *Sci. Rep.* **6**, 38361 (2016).
3. A. M. Peters van Ton, M. Kox, W. F. Abdo, P. Pickkers, Precision immunotherapy for sepsis. *Front. Immunol.* **9**, 1926 (2018).
4. P. H. Leliefeld, C. M. Wessels, L. P. Leenen, L. Koenderman, J. Pillay, The role of neutrophils in immune dysfunction during severe inflammation. *Crit. Care* **20**, 73 (2016).
5. A. D. Luster, Chemokines–Chemotactic cytokines that mediate inflammation. *N. Engl. J. Med.* **338**, 436–445 (1998).
6. O. Lindemann *et al*., TRPC1 regulates fMLP-stimulated migration and chemotaxis of neutrophil granulocytes. *Biochim. Biophys. Acta* **1853**, 2122–2130 (2015).
7. J. T. Mandeville, F. R. Maxfield, Effects of buffering intracellular free calcium on neutrophil migration through three-dimensional matrices. *J. Cell. Physiol.* **171**, 168–178 (1997).

8. E. J. Pettit, F. S. Fay, Cytosolic free calcium and the cytoskeleton in the control of leukocyte chemotaxis. *Physiol. Rev.* **78**, 949–967 (1998).
9. K. Itagaki *et al*., Store-operated calcium entry in human neutrophils reflects multiple contributions from independently regulated pathways. *J. Immunol.* **168**, 4063–4069 (2002).
10. V. M. Bolotina, Store-operated channels: Diversity and activation mechanisms. *Sci. STKE* **2004**, pe34 (2004).
11. K. Itagaki *et al*., Formyl peptide receptor-1 blockade prevents receptor regulation by mitochondrial danger-associated molecular patterns and preserves neutrophil function after trauma. *Crit. Care Med.* **48**, e123–e132 (2020).
12. E. Kaczmarek *et al*., A subset of five human mitochondrial formyl peptides mimics bacterial peptides and functionally deactivates human neutrophils. *J. Trauma Acute Care Surg.* **85**, 936–943 (2018).
13. K. Timmermans *et al*., Plasma levels of danger-associated molecular patterns are associated with immune suppression in trauma patients. *Intensive Care Med.* **42**, 551–561 (2016).
14. Q. Zhang *et al*., Circulating mitochondrial DAMPs cause inflammatory responses to injury. *Nature* **464**, 104–107 (2010).
15. S. Sun *et al*., Mitochondrial DAMPs increase endothelial permeability through neutrophil dependent and independent pathways. *PLoS One* **8**, e59989 (2013).
16. K. Pittman, P. Kubes, Damage-associated molecular patterns control neutrophil recruitment. *J. Innate Immun.* **5**, 315–323 (2013).
17. Y. Le, J. J. Oppenheim, J. M. Wang, Pleiotropic roles of formyl peptide receptors. *Cytokine Growth Factor Rev.* **12**, 91–105 (2001).
18. I. Migeotte, D. Communi, M. Parmentier, Formyl peptide receptors: A promiscuous subfamily of G protein-coupled receptors controlling immune responses. *Cytokine Growth Factor Rev.* **17**, 501–519 (2006).
19. X. Wang, W. Qin, Y. Zhang, H. Zhang, B. Sun, Endotoxin promotes neutrophil hierarchical chemotaxis via the p38-membrane receptor pathway. *Oncotarget* **7**, 74247–74258 (2016).
20. F. Bednar, C. Song, G. Bardi, W. Cornwell, T. J. Rogers, Cross-desensitization of CCR1, but not CCR2, following activation of the formyl peptide receptor FPR1. *J. Immunol.* **192**, 5305–5313 (2014).
21. H. Li *et al*., Mitochondrial damage-associated molecular patterns from fractures suppress pulmonary immune responses via formyl peptide receptors 1 and 2. *J. Trauma Acute Care Surg.* **78**, 272–279, discussion 279–281 (2015).
22. C. Zhao *et al*., Mitochondrial damage-associated molecular patterns released by abdominal trauma suppress pulmonary immune responses. *J. Trauma Acute Care Surg.* **76**, 1222–1227 (2014).
23. M. Bauer *et al*., Deterioration of organ function as a hallmark in sepsis: The cellular perspective. *Front. Immunol.* **9**, 1460 (2018).
24. B. Casserly *et al*., Lactate measurements in sepsis-induced tissue hypoperfusion: Results from the surviving sepsis campaign database. *Crit. Care Med.* **43**, 567–573 (2015).
25. R. S. Hotchkiss *et al*., Sepsis and septic shock. *Nat. Rev. Dis. Primers* **2**, 16045 (2016).
26. E. P. Rivers *et al*., The influence of early hemodynamic optimization on biomarker patterns of severe sepsis and septic shock. *Crit. Care Med.* **35**, 2016–2024 (2007).
27. G. M. Whitesides, E. Ostuni, S. Takayama, X. Jiang, D. E. Ingber, Soft lithography in biology and biochemistry. *Annu. Rev. Biomed. Eng.* **3**, 335–373 (2001).
28. B. Konecna *et al*., Monocyte exocytosis of mitochondrial danger-associated molecular patterns in sepsis suppresses neutrophil chemotaxis. *J. Trauma Acute Care Surg.* **90**, 46–53 (2021).
29. J. Demaret *et al*., Marked alterations of neutrophil functions during sepsis-induced immunosuppression. *J. Leukoc. Biol.* **98**, 1081–1090 (2015).
30. F. F. Larsen, J. A. Petersen, Novel biomarkers for sepsis: A narrative review. *Eur. J. Intern. Med.* **45**, 46–50 (2017).
31. C. N. Jones *et al*., Spontaneous neutrophil migration patterns during sepsis after major burns. *PLoS One* **9**, e114509 (2014).
32. C. Gemperle *et al*., Regulation of the formyl peptide receptor 1 (FPR1) gene in primary human macrophages. *PLoS One* **7**, e50195 (2012).
33. S. Agarwal, J. B. Suzuki, A. E. Riccelli, Role of cytokines in the modulation of neutrophil chemotaxis in localized juvenile periodontitis. *J. Periodontal Res.* **29**, 127–137 (1994).
34. J. A. Pedit, R. B. Marx, C. T. Miller, M. D. Aitken, Quantitative analysis of experiments on bacterial chemotaxis to naphthalene. *Biotechnol. Bioeng.* **78**, 626–634 (2002).
35. W. Zhao, H. Zhao, M. Li, C. Huang, Microfluidic devices for neutrophil chemotaxis studies. *J. Transl. Med.* **18**, 168 (2020).
36. P. V. Afonso *et al*., LTB4 is a signal-relay molecule during neutrophil chemotaxis. *Dev. Cell* **22**, 1079–1091 (2012).
37. S. Harbarth *et al*.; Geneva Sepsis Network, Diagnostic value of procalcitonin, interleukin-6, and interleukin-8 in critically ill patients admitted with suspected sepsis. *Am. J. Respir. Crit. Care Med.* **164**, 396–402 (2001).
38. V. Pettilä, M. Hynninen, O. Takkunen, P. Kuusela, M. Valtonen, Predictive value of procalcitonin and interleukin 6 in critically ill patients with suspected sepsis. *Intensive Care Med.* **28**, 1220–1225 (2002).
39. E. Kolaczkowska, P. Kubes, Neutrophil recruitment and function in health and inflammation. *Nat. Rev. Immunol.* **13**, 159–175 (2013).
40. T. Rimmelé *et al*.; ADQI XIV Workgroup, ADQI XIV Workgroup. Immune cell phenotype and function in sepsis. *Shock* **45**, 282–291 (2016).
41. M. Gossez *et al*., Proof of concept study of mass cytometry in septic shock patients reveals novel immune alterations. *Sci. Rep.* **8**, 17296 (2018).
42. Y. Le, P. M. Murphy, J. M. Wang, Formyl-peptide receptors revisited. *Trends Immunol.* **23**, 541–548 (2002).
43. American Thoracic Society; Infectious Diseases Society of America, Guidelines for the management of adults with hospital-acquired, ventilator-associated, and healthcare-associated pneumonia. *Am. J. Respir. Crit. Care Med.* **171**, 388–416 (2005).
44. M. Singer *et al*., The third international consensus definitions for sepsis and septic shock (Sepsis-3). *JAMA* **315**, 801–810 (2016).
45. Centers for Disease Control and Prevention, *National Healthcare Safety Network (NHSN) Patient Safety Component Manual* (Centers for Disease Control and Prevention, Atlanta, GA, 2019).
46. K. Wenzel-Seifert, R. Seifert, Cyclosporin H is a potent and selective formyl peptide receptor antagonist. Comparison with N-t-butoxycarbonyl-L-phenylalanyl-L-leucyl-L-phenylalanyl-L- leucyl-L-phenylalanine and cyclosporins A, B, C, D, and E. *J. Immunol.* **150**, 4591–4599 (1993).
47. M. H. Tarlowe *et al*., Inflammatory chemoreceptor cross-talk suppresses leukotriene B4 receptor 1-mediated neutrophil calcium mobilization and chemotaxis after trauma. *J. Immunol.* **171**, 2066–2073 (2003).
48. M. H. Tarlowe *et al*., Prospective study of neutrophil chemokine responses in trauma patients at risk for pneumonia. *Am. J. Respir. Crit. Care Med.* **171**, 753–759 (2005).
49. M. B. Hampton, M. C. Vissers, C. C. Winterbourn, A single assay for measuring the rates of phagocytosis and bacterial killing by neutrophils. *J. Leukoc. Biol.* **55**, 147–152 (1994).